16th World Conference on Earthquake, 16WCEE 2017
Santiago Chile, January 9th to 13th 2017
Paper N° 2211 (Abstract ID)
Registration Code: S-O1465484377

PARAMETER SENSITIVITY ANALYSIS OF THE MANZARI-DAFALIAS MODEL FOR MODELLING THE CYCLIC RESPONSE OF A SAND

L. Miranda[(1)], A. Barbosa[(2)], J. Serra[(3)], L. Caldeira[(4)]

[(1)] P.E., M.Sc., Laboratório Nacional de Engenharia Civil, lmiranda@lnec.pt
[(2)] P.E., Ph.D., Oregon State University, andre.barbosa@oregonstate.edu
[(3)] P.E., Ph.D., Laboratório Nacional de Engenharia Civil, biles@lnec.pt
[(4)] P.E., Ph.D., Laboratório Nacional de Engenharia Civil, laurac@lnec.pt

Abstract

In this paper, the numerical work that has been done to calibrate the Manzari-Dafalias model and to identify its more relevant parameters is presented. The model parameters, their respective reference values and the tests that were performed to determine most of the parameters are introduced. A parameter sensitivity analysis through numerical simulation of a triaxial monotonic drained test, using an OpenSees model with a single 1x1x1 m^3 SSPbrickUP 3D element, is described and the results analyzed. The sensitivity analysis is conducted for each parameter individually, for several pairs of physically related parameters and of the most relevant ones. It is considered the final influence upon the peak values of the shear strain ε_s, shear stress ratio η and dilatancy and upon the critical state volumetric strain ε_v.

Furthermore, a parameter sensitivity analysis through numerical simulation of a cyclic undrained torsional test is implemented, both for the pre-liquefaction and liquefaction phases. In the former, the variation of some response parameters (namely the damping ratio, the shear modulus, the shear stress amplitude, the average shear stress, the shear strain amplitude and the average p) with the model parameters is evaluated for three different cycles.

Keywords: Sand, Manzari-Dafalias model, Sensitivity analysis, Triaxial test, Torsional test, Liquefaction

1. Introduction

The Manzari-Dafalias (M-D) constitutive model [1, 2] is capable of realistically simulating the stress-strain behavior of sands under monotonic and cyclic loads with drained or undrained conditions. It allows defining a unique set of model parameters for a given sand, independent of soil density and confining pressure values. This model is effective in reproducing relevant aspects of soil response under cyclic loading including liquefaction triggering (contraction tendency with pore pressure buildup) and dilatancy effects. It is quite relevant that the post-liquefaction behavior is also well reproduced, as large shear and volumetric deformations in saturated sands are found to take place mainly after liquefaction, eventually causing heavy damage in structures.

The design of a third Tagus river crossing is currently being considered downstream of 25 de Abril Bridge in Lisbon, Portugal. This corresponds to an immersed tunnel with a length of approximately 2.4 km, which is supported by alluvial Tagus basin sands, overlaying Miocenic layers of increasing stiffness and strength in depth, and basalt bedrock. The potential occurrence of seismically induced liquefaction in the foundation ground and the prescription of efficient preventive measures are topics of utmost importance within this project. Being the M-D model a natural candidate for numerical modelling of the problem, this paper addresses its applicability to the referred goal.

While the model can be effective and has been shown to produce good results, the calibration of its large number of parameters can be cumbersome. This paper summarizes the numerical work to calibrate the M-D model to the estuarine sand properties in order to facilitate its application in the scope of the Tagus crossing.

The calibration framework presented for the M-D model combines results of laboratory tests with numerical sensitivity studies. Many of the model parameters, specifically those related to the monotonic behavior, are calibrated directly from triaxial monotonic drained tests (TMDT). The remaining parameters, related to the monotonic and cyclic behavior, are calibrated through numerical simulation of laboratory tests (TMDT and cyclic undrained torsional tests – CUTT, respectively). A constitutive driver developed in OpenSees is used to perform the simulations. A parameter sensitivity analysis is carried out in order to better understand the relevance of each model parameter. All stresses herein defined are effective stresses.

2. The Manzari-Dafalias model and parameter reference values

This model builds upon previous work by Manzari and Dafalias [1], in which the two-surface formulation of plasticity is coupled with a state parameter to construct a constitutive model for sands in a general stress space. This work was extended to account for the effect of fabric changes during loading [2]. It was observed that, despite the bounding surface formulation, the simulation of reverse loading was not very accurate for small values of the effective stress. This is attributed to the fact that the model did not account for the drastic change in fabric observed in microscopic studies during the dilatant phase of plastic strain, which has a significant effect on the contracting response upon reversal of loading. The latter is considered to be key to successfully simulate the effective stress reduction and modulus degradation under undrained cyclic loading. Thus, the dilatancy is made to depend on a fabric-dilatancy tensor whose evolution models macroscopically the foregoing phenomenon of fabric changes and their effect on dilatancy characteristics.

In the formulation in triaxial stress space, the **critical state**, for which the soil deforms continuously in shear with no volume change, can be defined by the critical state stress ratio $q_c/p_c = M_{f,c}$, where the parameter $M_{f,c}$ is uniquely related to the friction angle ϕ_f.The power relation suggested in [3] is used for the equation of the critical state line in e-p space $e_c = e_c(p_c)$.

$$e_c = e_{p0} - \lambda_c (p_c/p_a)^{\xi} \tag{1}$$

with e_{p0} the void ratio at $p_c = 0$, p_a the atmospheric pressure and λ_c and ξ constants.

To define the critical state in extension, the parameter c is introduced:

$$c = \frac{M_{f,e}}{M_{f,c}} \tag{2}$$

The **yield surface** represents a ''wedge'' in *p*-*q* space, whose bisecting line has a slope α, and the wedge opening a value of $2mp$ (Fig. 1). It is defined as

$$f = |\eta - \alpha| - m = 0 \tag{3}$$

α and m are stress ratio quantities. The model considers isotropic and kinematic hardening. If m is fixed, then α can be related with the plastic hardening modulus H_p through $d\alpha = H_p d\varepsilon_q^p$.

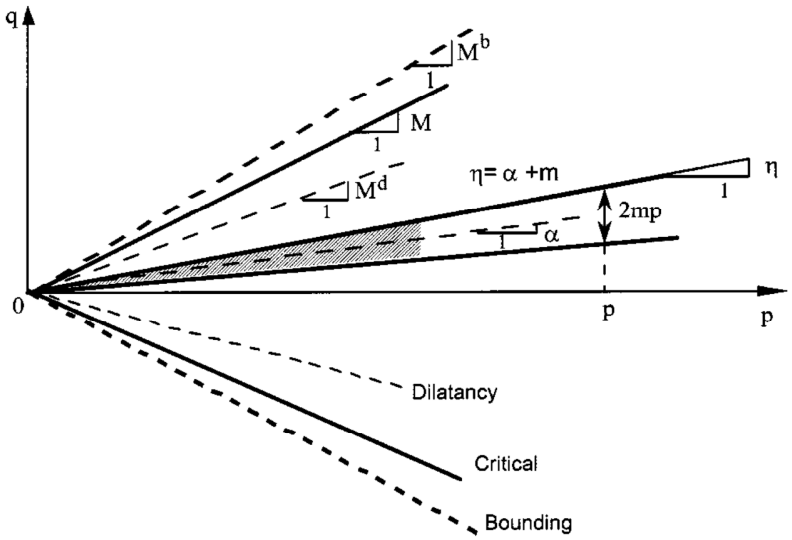

Fig. 1 – Yield, critical, dilatancy and bounding lines in *q*, *p* space [2]

The **plastic hardening modulus H_p** depends on the distance $b = M^b \mp \eta$ where M^b is a peak or bounding stress ratio, which bounds the compression (-) or extension (+) loading, when it increases under monotonic drained triaxial compression or extension. For the simplest case of linear dependence:

$$H_p = h\left(M^b \mp \eta\right) \tag{4}$$

where positive h is a function of the state variables, given by:

$$h = \frac{b_0}{|\eta - \eta_{in}|};\ \ b_0 = G_0 h_0 (1 - c_h e) \left(\frac{p}{p_a}\right)^{-1/2} \tag{5}$$

with scalar parameters h_0 and c_h. η_{in} is the value of η at initiation of a loading process in compression or the value of h at the point of reversal in extension. Thus, during loading with $d\eta > 0$ one has $H_p = h\left(M^b - \eta\right)$, while for reverse loading with $d\eta < 0$ it changes to $H_p = h\left(M^b + \eta\right)$.

According to Rowe's theory, dilatancy d becomes proportional to the difference of current stress ratio η from dilatancy stress ratio M^d, which is also defined as the **phase transformation line** [4]:

$$d = A_d\left(M^d - \eta\right) \tag{6}$$

Depending on $\eta < M^d, \eta > M^d$ or $\eta = M^d$ a contractant ($d > 0$), dilatant ($d < 0$) or zero volumetric rate ($d = 0$) response is obtained. A corresponding dilatancy stress ratio M^d in extension can be defined, so that $d = A_d\left(M^d + \eta\right)$ in a similar way to the bounding stress ratio M^d.

Let a **fabric-dilatancy** internal variable z that evolves according to:

$$dz = -c_z\langle -d\varepsilon_v^p\rangle(sz_{max} + z) \tag{7}$$

be introduced. Parameter A_d is given by:

$$A_d = A_0(1 + \langle sz\rangle) \tag{8}$$

where $\langle x\rangle = x$ if $x > 0$ and $\langle x\rangle = 0$ if $x \leq 0$ and $s = \pm 1$ according to $\eta = \alpha \pm m$, respectively.

Before fabric-dilatancy is activated one has $A_0 = A_d$. Thus, to determine the parameter A_0, a constant p test is made. Then, based on the test results, dilatancy $d = -\frac{\delta\varepsilon_v}{\delta\varepsilon_q}$ is determined, as well as the corresponding values of η. Finally, using Eq. (6), a linear regression is made at the dilatancy zone just before the peak to obtain the value of A_0.

In order that the constitutive relations are compatible with critical state soil mechanics requirements and can simulate softening of dense sands, an appropriate variation of M^b and M^d with the material state was also considered in [2], such that when $e = e_c$ and $p = p_c$, then $M^b = M^d = M_{f,c}$. Furthermore, for states denser than critical ($e < e_c$), the condition $M^d < M_{f,c} < M^b$ must hold, and the reverse for states looser than critical. Along these lines, the use of the following equations was proposed in [5]:

$$M^b = M_{f,c} exp(-n^b \Psi) \tag{9}$$

$$M^d = M_{f,c} exp(n^d \Psi) \tag{10}$$

with n^b and n^d material constants.

Both n^b and n^d are determined making an average of the values obtained for 3 different confining pressures (100, 200 and 300 kPa) and using Eq. (9) and Eq. (10), respectively. Where $M^b = \eta_{peak}$ (peak state) and $M^d = \eta_{\Delta V=0}$ (state where the volumetric change is zero). $\Psi = e - e_c$, where $e^b = e_{peak}$ and $e^d = e_{\Delta V=0}$.

In conclusion, for the Tagus sand the following parameters of the M-D model were directly determined from triaxial monotonic drained tests: $M_{f,c} = 1.46$, $c = 0.67$, $e_{p0} = 0.014$, $\lambda_c = 0.78$ and $\xi = 1.15$ (related with the critical state); $n^b = 3.5$ (related with the plastic modulus) and $A_0 = 0.932$ and $n^d = 1.5$ (related with dilatancy).

These model parameters and respective reference values, which correspond either to laboratory tests results ([lab] in Table 1) or to published data in several references about the M-D model [2, 6, 7, 8], as well as the tests commonly used to determine the parameters are summarized in Table 1. Apart from the laboratory determined properties of the estuarine sand, for the sensitivity analysis it was considered a variation of ±20% of the reference value (except for parameter m – 0.015, 0.03, 0.06).

Both the calibration framework and the sensitivity analysis results presented here provide modelers with an understanding of the effects of modeling parameters on model performance. The parameters selected for the sensitivity analysis are the ones that couldn't be obtained directly by laboratory tests (G_0, m, h_0 and c_h) as well as some parameters that, though obtained directly through laboratory tests, don't have a straight physical meaning (n^b, A_0 and n^d). The intrinsic (physical and critical state parameters) weren't considered for the sensitivity analysis.

3. Parameter sensitivity analysis through numerical simulation of triaxial monotonic drained test

In order to perform this sensitivity analysis it was built an OpenSees model [6], using a single 1x1x1 m^3 SSPbrickUP 3D element with 8 nodes. It can be used in dynamic 3D analysis of fluid saturated porous media with a mixed displacement-pressure ($u - p$) formulation, based upon the work of Biot as extended by Zienkiewicz and Shiomi [9].

Regarding boundary conditions, at the base of the element two of the 4 nodes were free in each horizontal direction (x and y) and one was free in both horizontal directions. The top nodes were all free. During the consolidation phase concentrated forces representing an all-around pressure were applied on the free nodes at the base and top of the element, corresponding to the chosen confining pressures p_{conf} (100, 200 and 300 kPa). For the shear phase of the triaxial test, a vertical displacement (z) was applied at the four nodes of the top face of the element, until a vertical axial strain of approximately 20% was reached.

Table 1 – *Manzari-Dafalias* model parameters, reference values and published data ([6, 7, 8])

Category	Parameter	Reference value	Test
Physical	ρ_s (kN/m^3)	16.21 [lab]	Physical testing
	e_0	0.634 [lab]	Physical testing (Dr = 71.3%)
Elasticity	G_0	125 [6]	RC (though values from small strain measurements may be 2 or 3 times too large)
	ν	0.3 [lab] ($\phi = 36°$)	$\nu = \frac{K_0}{1+K_0}$; $K_0 = 1 - \sin\phi$ (0.2 to 0.4 in [7])
Critical state	$M_{f,c}$	1.46 [lab]	TMDT (1.20 to 1.32 in [7])
	c	0.67 [lab]	TMDT (using $M_{f,c}$ and $M_{f,e}$)
	λ_c	0.014 [lab]	TMDT that approach critical state (0.01 to 0.03 in [7])
	e_{p0}	0.78 [lab]	Void ratio at $p_c = 1$ kPa. TMDT that approach critical state (0.72 to 0.90 in [7])
	ξ	1.15 [lab]	TMDT that approach critical state ($\xi = 0.7$ for most sands [8])
Yield surface	m	0.015 [6]	Fitting (TMDT) (0.06-0.07 in [7], 0.02-0.05 in [8]).
Plastic modulus	h_0	7.05 [6]	Fitting (TMDT)
	c_h	0.968 [6]	Fitting (TMDT)
	n^b	3.5 [lab]	$n^b = \ln(\frac{M}{M^b})/\Psi^b$, where Ψ^b and M^b are the values of Ψ and η at a drained peak stress state (1.1 in [2])
Dilatancy	A_0	0.932 [lab]	TMDT – good quality stress dilatancy data – volumetric strain vs. deviatoric strain in a constant p drained triaxial test (before z is activated $A_0 = A_d$) (0.704 in [2])
	n^d	1.5 [lab]	$n^d = \ln(\frac{M}{M^d})/\Psi^d$, where Ψ^d and M^d are the values of Ψ and η at a phase transformation state (3.5 in [2])
Fabric-dilatancy tensor	z_{max}	4 [6]	Fitting (CUTT) – η must exceed M^d so that the evolution of z is activated (4-5 for most sands according to [8])
	c_z	600 [6]	Fitting (CUTT) - η must exceed M^d so that the evolution of z is activated

TMDT – monotonic drained triaxial test; RC – resonant column test; CUTT – cyclic undrained torsional test.

3.1 Sensitivity analysis for each model parameter

In Table 2, the results for a 200 kPa confining pressure are summarized. The sensitivity analysis of the individual parameters points out that the model parameters that cause a greater variation of the response are: c_h concerning peak shear strain ε_s, n^b regarding peak shear stress ratio η and finally A_0 concerning peak dilatancy and volumetric strain at critical state ε_V. Similar conclusions may be drawn from the 100 and 300 kPa simulations.

Fig. 2 to Fig. 4 present the $\eta\ vs.\ \delta\varepsilon_s$ graphic and the relation between the volumetric strain $\delta\varepsilon_V$ and the shear strain $\delta\varepsilon_s$ considering, respectively, the variation of the parameters c_h, n^b and A_0 in the response.

Table 2 – Parameter sensitivity analysis of TMDT (confining pressure of 200 kPa)

parameters	η (peak)	ε_s (peak)	dilatancy (peak)	ε_V (critical)
Reference case	1.782	3.028%	0.410	-4.071%
$G_0 = 100$	1.783	3.608%	0.411	-4.051%
$G_0 = 150$	1.781	2.637%	0.411	-4.085%
$m = 0.03$	1.782	3.023%	0.412	-4.072%
$m = 0.06$	1.782	2.966%	0.411	-4.073%
$h_0 = 5.50$	1.774	3.586%	0.401	-4.069%
$h_0 = 8.50$	1.787	2.684%	0.417	-4.073%
$c_h = 0.75$	1.790	2.496%	0.422	-4.070%
$c_h = 1.15$	1.771	3.829%	0.400	-4.081%
$n^b = 2.8$	1.732	3.264%	0.372	-3.865%
$n^b = 4.2$	1.825	2.843%	0.446	-4.223%
$A_0 = 0.75$	1.788	3.173%	0.336	-3.667%
$A_0 = 1.10$	1.777	2.917%	0.479	-4.331%
$n^d = 1.2$	1.785	3.071%	0.391	-3.971%
$n^d = 1.8$	1.778	3.014%	0.429	-4.160%

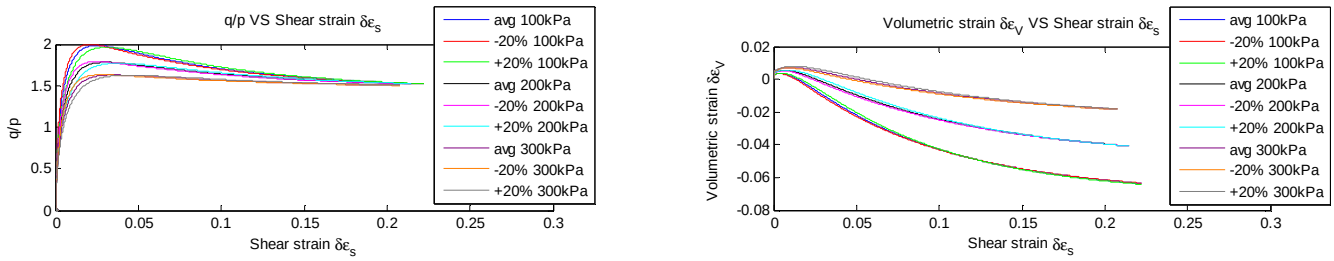

Fig. 2 – Simulation results considering c_h variation

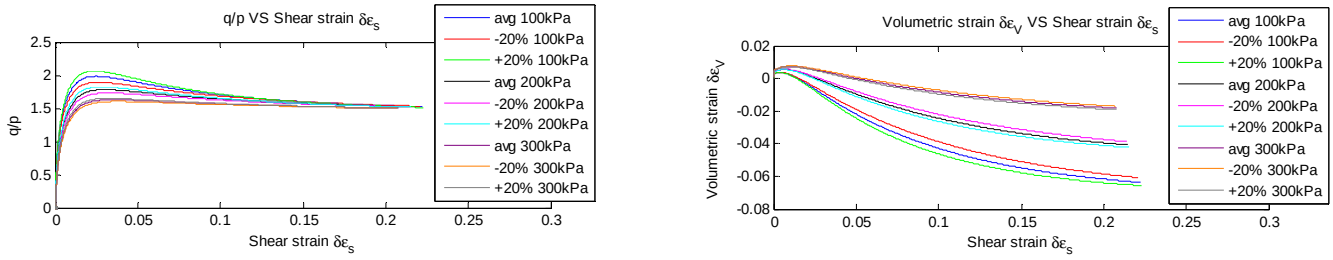

Fig. 3 – Simulation results considering n^b variation

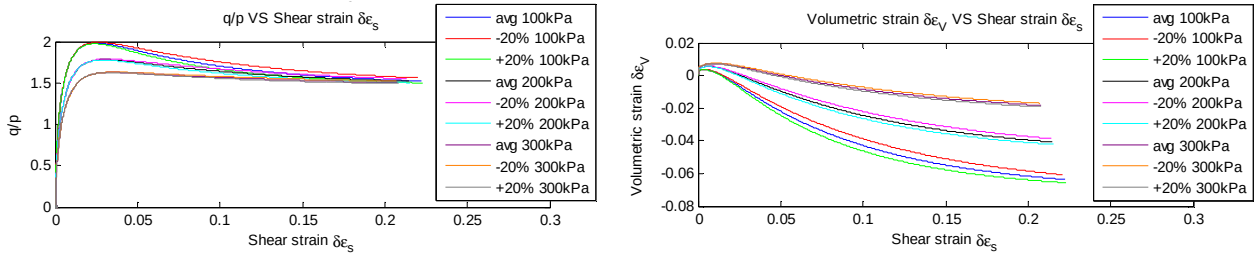

Fig. 4 – Simulation results considering A_0 variation

3.2 Sensitivity analysis for model related parameters (A_0 with n^d and c_h with h_0)

Then, two related parameters (A_0 and n^d concern dilatancy while c_h and h_0 regard the plasticity modulus) were varied simultaneously, according to Table 3, for a confining pressure of 200 kPa. Observing both Table 2 and Table 3 it can be concluded that, when the parameters c_h and h_0 are varied simultaneously, the ε_s variation is fairly greater than when only one of the parameters is changed. In the case of A_0 and n^d the variation of the response is only slightly larger than when only one of the parameters is changed.

Table 3 – Two related parameter sensitivity analysis of TMDT (confining pressure of 200 kPa)

Parameters	η (peak)	ε_s (peak)	dilatancy (peak)	ε_V (critical)
Reference case	1.782	3.035%	0.411	-4.071%
$A_0 = 0.75$; $n^d = 1.2$	1.791	3.226%	0.322	-3.551%
$A_0 = 0.75$; $n^d = 1.8$	1.785	3.149%	0.352	-3.773%
$A_0 = 1.10$; $n^d = 1.2$	1.781	2.974%	0.349	-4.247%
$A_0 = 1.10$; $n^d = 1.8$	1.773	2.907%	0.348	-4.403%
$c_h = 0.75$; $h_0 = 5.50$	1.783	2.935%	0.412	-4.067%
$c_h = 0.75$; $h_0 = 8.50$	1.794	2.207%	0.424	-4.072%
$c_h = 1.15$; $h_0 = 5.50$	1.763	4.523%	0.361	-4.083%
$c_h = 1.15$; $h_0 = 8.50$	1.777	3.372%	0.400	-4.080%

Fig. 5 presents the $\eta\ vs.\ \delta\varepsilon_s$ graphic and the relation between the volumetric strain $\delta\varepsilon_V$ and the shear strain $\delta\varepsilon_s$ considering the four cases of variation of c_h and h_0 described in Table 3.

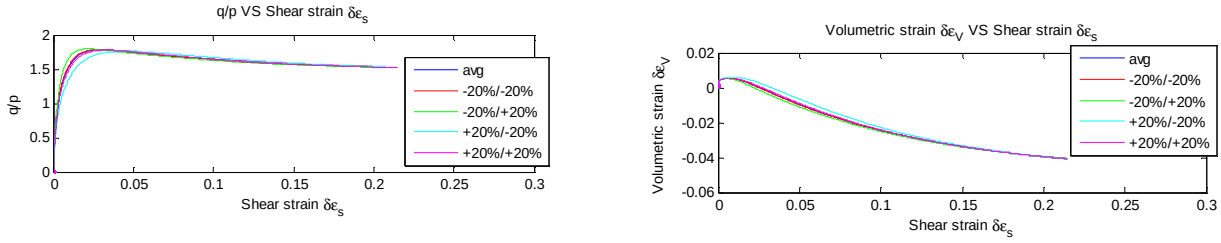

Fig. 5 – Simulation results considering simultaneous variation of c_h and h_0

3.3 Sensitivity analysis for the most relevant parameters (A_0 with c_h, A_0 with n^b and c_h with n^b)

Finally, pairs of the most relevant parameters (c_h, n^b and A_0) determined in 3.1 are varied simultaneously. The results of the sensitivity analysis for a confining pressure of 200 kPa are presented in Table 4.

The analysis of both Table 2 and Table 4 shows that the joint variations of parameters c_h and A_0 causes larger variation than when only one of the parameters is changed. In the case of A_0 and n^b and A_0 and c_h the effect on η (peak) is only slightly larger to when one of the parameters is independently changed. This also happens when analysing ε_s after changing simultaneously c_h and n^b.

Fig. 6 presents the $\eta\ vs.\ \delta\varepsilon_s$ graphic and the relation between the volumetric strain $\delta\varepsilon_V$ and the shear strain $\delta\varepsilon_s$ considering the four cases of variation of c_h and A_0 described in Table 4.

In a nutshell, the most important parameters to consider in a sensitivity analysis are c_h, $n^b$and A_0. In a joint sensitivity analysis c_h and h_0 shall be varied simultaneously, as well as c_h and A_0.

Table 4 – Two most relevant parameter sensitivity analysis of TMDT (confining pressure of 200 kPa)

Parameters	η (peak)	ε_s (peak)	dilatancy (peak)	ε_V (critical)
Reference case	1.782	3.035%	0,411	-4.071%
$A_0 = 0.75$ / $c_h = 0.75$	1.795	2.597%	0,343	-3.673%
$A_0 = 0.75$ / $c_h = 1.15$	1.778	4.007%	0,327	-3.662%
$A_0 = 1.10$ / $c_h = 0.75$	1.785	2.418%	0,277	-4.325%
$A_0 = 1.10$ / $c_h = 1.15$	1.765	3.682%	0,327	-4.351%
$A_0 = 0.75$ / $n^b = 2.8$	1.737	3.409%	0,305	-3.435%
$A_0 = 0.75$ / $n^b = 4.2$	1.832	2.973%	0,362	-3.846%
$A_0 = 1.10$ / $n^b = 2.8$	1.728	3.162%	0,366	-4.155%
$A_0 = 1.10$ / $n^b = 4.2$	1.820	2.748%	0,361	-4.456%
$c_h = 0.75$ / $n^b = 2.8$	1.739	2.673%	0,382	-3.871%
$c_h = 0.75$ / $n^b = 4.2$	1.834	2.349%	0,456	-4.217%
$c_h = 1.15$ / $n^b = 2.8$	1.723	4.150%	0,402	-3.862%
$c_h = 1.15$ / $n^b = 4.2$	1.813	3.563%	0,437	-4.242%

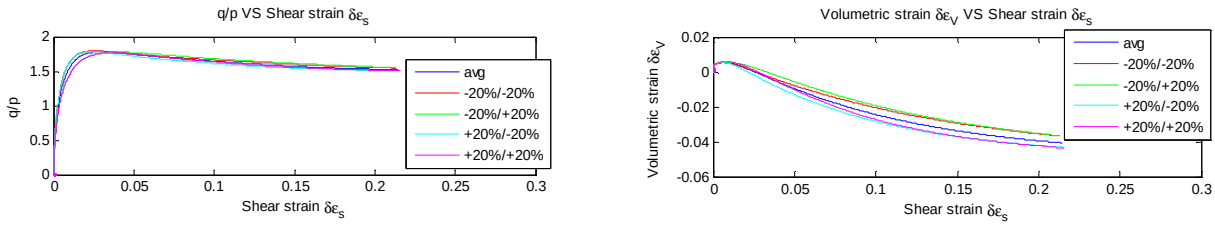

Fig. 6 – Simulation results considering simultaneous variation of c_h and A_0

4. Parameter sensitivity analysis through numerical simulation of cyclic undrained torsional test

In this case, the consolidation phase of the test is modeled similarly to the triaxial test described in section 3. Then, in order to simulate the shear phase of the cyclic undrained torsional test, the pore pressure is set free at the nodes of the element. The nodes of the top of the element are fixed in the horizontal direction (y). Displacements are applied at all four top nodes in the x horizontal direction, according to a sine cyclic function, with a frequency of 1 Hz and which amplitude increases progressively up to 0.03 m ($1x10^{-5}$, $5x10^{-5}$, $1x10^{-4}$, $5x10^{-4}$, 0.001, 0.003, 0.006, 0.01, 0.02 and 0.03 m).

4.1 Sensitivity analysis in the pre-liquefaction phase

The sensitivity analysis was performed for three different confinement pressures: 100, 200 and 300 kPa.

Table 5 and Table 6 show the variation of some response parameters (namely the damping ratio ξ, the shear modulus, the shear stress amplitude, the average shear stress, the shear strain amplitude and the average p) with the model parameters G_0, m, h_0, c_h, n^b, A_0 and n^d for two different cycles and for a confining pressure of 200 kPa. It is important to refer that the parameters c_z and z_{max} don't affect the pre-liquefaction response, having influence only on the liquefaction response. The cells in red mean the variation in relation to the reference case was over 10%.

Table 5 – Sensitivity analysis of CUTT in the pre-liquefaction phase – cycle 1 (confining pressure of 200 kPa)

	ξ (%)	Shear modulus (kPa)	Shear stress amplitude (kPa)	Average shear stress (kPa)	Shear strain amplitude (%)	Average p (kPa)
Reference case	**1.9**	**52814**	**9.1**	**1.2**	**0.0173**	**179.6**
Pre-liquefaction parameters – Cycle 1	variation (%)	variation (%)	variation (%)	variation (%)	variation (%)	variation (%)
$G_0 = 100$	-22.07	-17.28	-15.11	1.41	2.31	3.41
$G_0 = 150$	30.98	15.23	15.00	-1.82	-0.58	-4.13
$m = 0.03$	-20.36	7.81	0.22	3.31	-7.51	7.39
$m = 0.06$	-99.94	13.35	0.33	4.88	-11.56	11.09
$h_0 = 5.50$	30.98	-2.06	-0.05	-0.50	1.73	-1.35
$h_0 = 8.50$	-17.24	1.02	0.03	0.25	-1.16	0.64
$c_h = 0.75$	-25.80	3.53	0.10	1.41	-3.47	2.99
$c_h = 1.15$	41.66	-5.74	-0.16	-2.32	5.78	-4.95
$n^b = 2.8$	9.38	-1.28	-0.03	-0.50	1.16	-1.08
$n^b = 4.2$	-8.49	1.16	0.03	0.50	-1.16	0.97
$A_0 = 0.75$	-2.07	1.29	0.03	0.08	-1.16	2.27
$A_0 = 1.10$	2.09	-1.23	-0.02	-0.08	1.16	-2.15
$n^d = 1.2$	0.44	-0.26	0.00	0.00	0.00	-0.46
$n^d = 1.8$	-0.40	0.25	0.01	0.00	-0.58	0.44

Table 6 – Sensitivity analysis of CUTT in the pre-liquefaction phase – cycle 3 (confining pressure of 200 kPa)

	ξ (%)	Shear modulus (kPa)	Shear stress amplitude (kPa)	Average shear stress (kPa)	Shear strain amplitude (%)	Average p (kPa)
Reference case	**14.9**	**12458**	**22.5**	**0.2**	**0. 1804**	**48.7**
Pre-liquefaction parameters – Cycle 3	variation (%)	variation (%)	variation (%)	variation (%)	variation (%)	variation (%)
$G_0 = 100$	0.61	-25.76	-19.16	-12.30	8.87	-18.22
$G_0 = 150$	8.67	51.06	-22.31	245.99	-48.56	-5.50
$m = 0.03$	13.92	48.20	4.50	282.35	-29.49	13.75
$m = 0.06$	98.87	18.74	95.26	683.42	64.41	42.37
$h_0 = 5.50$	17.77	22.70	3.01	415.51	-16.08	15.43
$h_0 = 8.50$	-0.91	36.25	2.93	102.67	-24.45	3.06
$c_h = 0.75$	12.75	31.59	3.74	247.06	-21.18	-12.16
$c_h = 1.15$	9.63	24.85	-33.89	219.25	-47.06	-1.60
$n^b = 2.8$	19.13	41.91	3.31	235.29	-27.22	27.34
$n^b = 4.2$	14.09	41.14	4.06	271.12	-26.27	4.90
$A_0 = 0.75$	17.96	-10.47	-1.31	-123.53	10.20	-13.31
$A_0 = 1.10$	9.21	44.59	4.30	345.99	-27.88	25.34
$n^d = 1.2$	33.99	32.99	3.98	325.67	-21.84	13.95
$n^d = 1.8$	3.35	36.07	2.96	140.64	-24.33	14.74

It can be observed that at the beginning of the shear phase (cycle 1), for the same parameter variation, the changes in the response are generally smaller than closer to liquefaction, where the shear strain is much higher (cycle 3). Nevertheless, in cycle 1 a variation of G_0, m, h_0 and c_h causes significant variation of the damping ratio, being c_h the most relevant. The variation of G_0 is also important regarding the average shear modulus and the shear stress amplitude. Concerning cycle 2, all the model parameters but n^d exert influence on the response, except for the shear stress amplitude, which is only influenced by G_0, and the average shear stress, that is mainly influenced by G_0, m, h_0 and c_h. These four parameters are also those which exercise a greater influence on the response. Finally, for cycle 3 all the model parameters but n^d have influence on the response, except for the shear stress amplitude which is only influenced by G_0 and c_h. Thus, from the global analysis of these tables, it can be concluded that the most relevant parameters for pre-liquefaction cyclic response are G_0, m, h_0 and c_h.

In Fig. 7, the shear stress-shear strain relation ($\tau_{xz}\ vs.\ \varepsilon_{xz}$) for the 3 cycles above described, the normalized stress path ($q/p_{conf}\ vs.\ p/p_{conf}$) for the pre-liquefaction phase and the pore pressure ratio variation during the shear phase are presented, considering the variation of the parameter G_0 in the response.

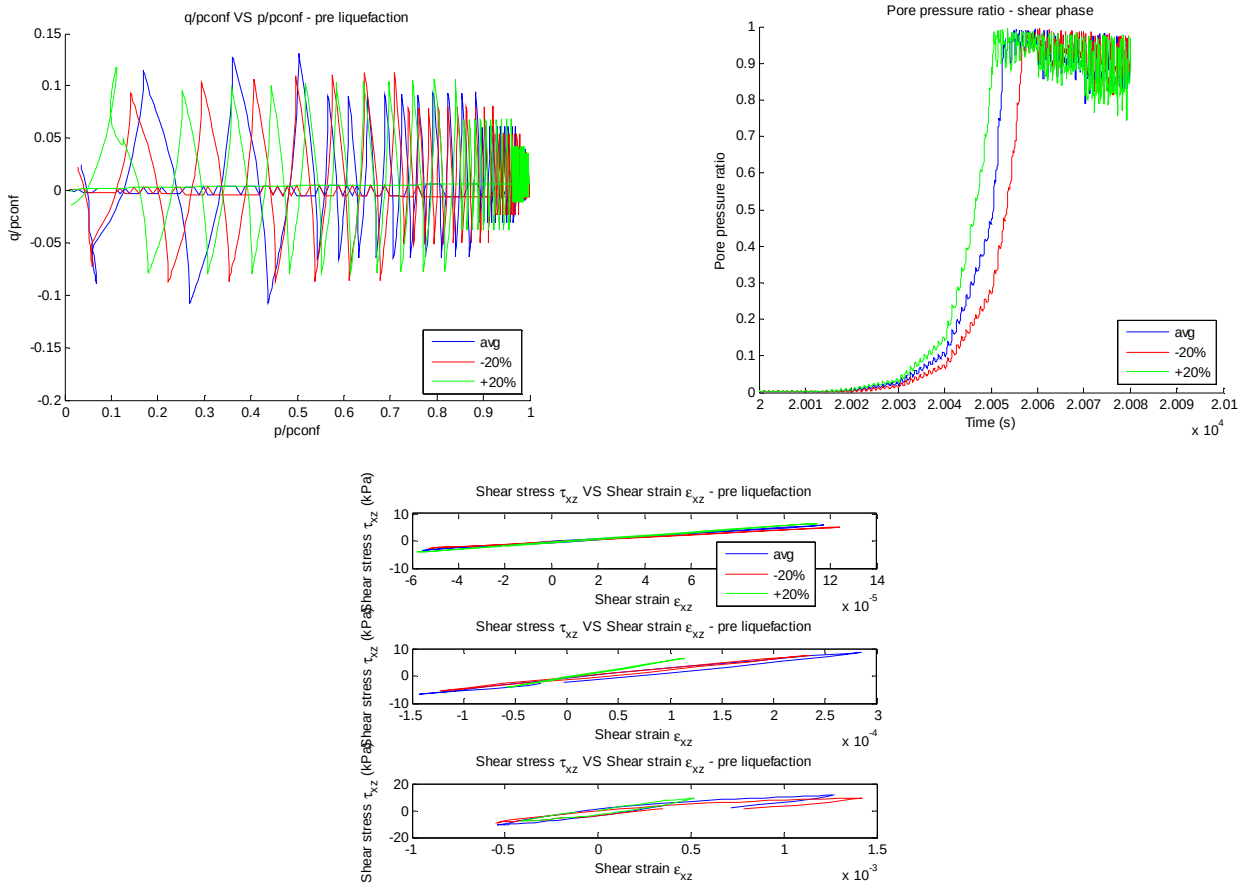

Fig. 7 – ($q/p_{conf}\ vs. p/p_{conf}$) and ($\tau_{xz}\ vs. \varepsilon_{xz}$) paths and pore pressure ratio time history considering variation of G_0

4.2 Sensitivity analysis in the liquefaction phase

In Fig. 8, the shear stress-shear strain relation ($\tau_{xz}\ vs. \varepsilon_{xz}$) for a chosen cycle in the liquefaction phase and the normalized stress path ($q/p_{conf}\ vs.\ p/p_{conf}$) for 3 cycles in the liquefaction phase are presented, considering the influence of the variation of c_z upon the response.

In the liquefaction phase, in each cycle, the pore pressure ratio should reach a value near one and the shear stress should be around zero at the same time. Moreover, the shear strain should follow the applied cyclic displacements. However, due to convergence problems of the M-D model, the pore pressure ratio varies significantly, with its maximum value decreasing and moving away from one, the shear stress doesn't reach zero and the shear strain doesn't follow the applied cyclic displacements (Fig. 8). Thus, it wasn't possible to determine the relative importance of these parameters in the cyclic response. Further improvements in the M-D numerical model are deemed necessary.

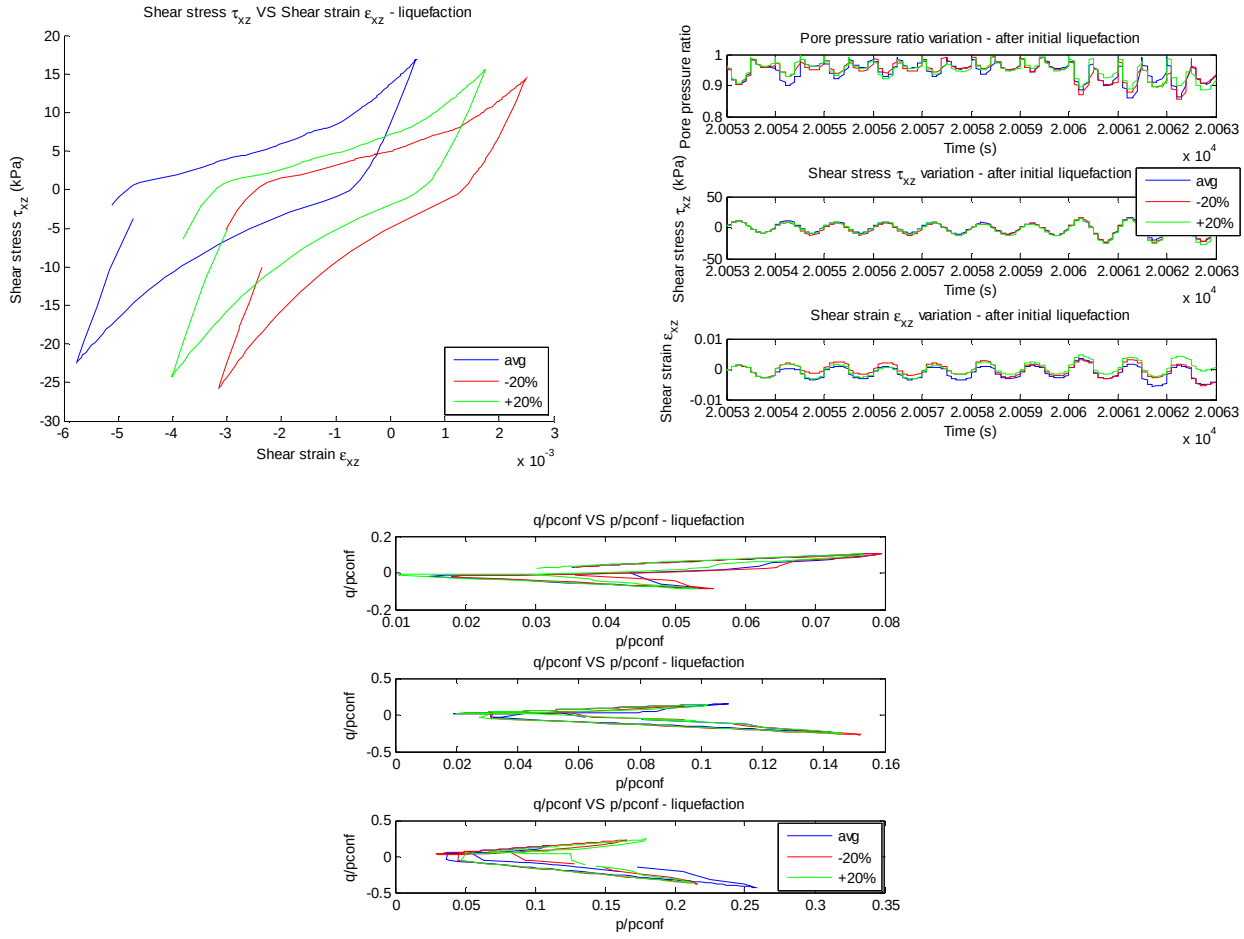

Fig. 8 – $(q/p_{conf}\ vs.\ p/p_{conf})$ and $(\tau_{xz}\ vs.\ \varepsilon_{xz})$ paths and pore pressure ratio time history considering variation of c_z

5. Concluding remarks

Based on a parameter sensitivity analysis through numerical simulation of a triaxial monotonic drained test, it was concluded that the model parameters that cause a greater variation of the response are: $\boldsymbol{c_h}$ concerning ε_s (peak), $\boldsymbol{n^b}$ regarding η (peak) and finally $\boldsymbol{A_0}$ in what concerns dilatancy (peak) and ε_V (critical). Moreover, when the parameters $\boldsymbol{c_h}$ **and** $\boldsymbol{h_0}$ are varied at the same time, the ε_s variation is reasonably greater than the variation induced by each parameter individually. Likewise, when the parameters $\boldsymbol{c_h}$ **and** $\boldsymbol{A_0}$ are varied together, the dilatancy variation is considerably greater than when only one of the parameters is changed.

Regarding the parameter sensitivity analysis through numerical simulation of a cyclic undrained torsional test in the pre-liquefaction phase, from the analysis of three cycles, corresponding to progressively higher shear strains (approaching liquefaction), it can be concluded that the most relevant parameters for pre-liquefaction cyclic response are $\boldsymbol{G_0}$, $\boldsymbol{m}$, $\boldsymbol{h_0}$ **and** $\boldsymbol{c_h}$. As to the liquefaction phase, due to convergence problems of the Manzari-Dafalias model in this phase, it wasn't yet possible to determine the relative importance of parameters c_z and z_{max} in the cyclic response.

6. Acknowledgements

Luís Miranda was supported by "Fundação para a Ciência e Tecnologia" (FCT – Portugal), through the PhD scholarship SFRH/BD/99581/2014.

The authors want to thank Pedro Arduino, Chris McGann and Deepak for their help and suggestions related with the numerical modelling of the triaxial and torsional tests.

7. References

[1] Manzari MT, Dafalias YF (1997). A critical state two-surface plasticity model for sands. *Geotechnique*, 255–272.

[2] Dafalias YF, Manzari MT (2004). Simple Plasticity Sand Model Accounting for Fabric Change Effects. *J Eng Mech* **130**, 622–634.

[3] Li X, Wang Y (1998). Linear Representation of Steady-State Line for Sand. *J Geotech Geoenviron Eng* **124**, 1215–1217.

[4] Ishihara K, Tatsuoka F, Yasuda S (1975). Undrained deformation and liquefaction of sand under cyclic stresses. *Soils and Foundations*, **15** (1), 29-44.

[5] Li XS, Dafalias YF (2000). Dilatancy for cohesionless soils. *Geotechnique* **50** (4):449–460.

[6] University of Berkeley, California. OpenSees (Open System for Earthquake Engineering Simulation). *http://OpenSees.berkeley.edu/*

[7] Papadimitriou AG, Bouckovalas GD, Dafalias YF (2001). Plasticity model for sand under small and large cyclic strains. *J Geotech Geoenvironmental Eng* **127**, 973–983.

[8] Cheng, Z., Dafalias Y.F., Manzari M.T. (2013). Application of SANISAND Dafalias-Manzari model in FLAC 3D. *In* Zhu, Detournay, Hart & Nelson (eds.), Continuum and Distinct Element Numerical Modeling in Geomechanics, Paper 09-03.

[9] Zienkiewicz, O.C. and Shiomi, T. (1984). Dynamic behavior of saturated porous media; the generalized Biot formulation and its numerical solution. *International Journal for Numerical Methods in Geomechanics* **8**, 71-96.